Electronic Supplementary Material (ESI) for ChemComm.

Supporting Information

The active site for the water oxidizing anodic iridium oxide probed through in-situ Raman Spectroscopy

1. Experimental Section

All the solutions were prepared from high purity reagents: H_2IrCl_6 (Alfa Aesar, 99%), NaOH (Fluka Analytical, 99.9995%), D_2O (Sigma-Aldrich, 99.9 atom % D), H_2O^{18} (Sercon, 98 atom % O^{18}), $HClO_4$ (Suprapur, 70 vol %), H_2SO_4 (Suprapur 98 vol %), NaCl (SAFC, 5 M solution). All solutions were prepared by using Millipore Milli-Q water (18.2 MΩ•cm). Au foil (Alfa Aesar Premion, 99.9975%, 0.1 mm) was used as the substrate, Ir foil (Advent Research Materials, 99.9%, 0.05 mm) was used for obtaining pure cyclic voltammogram of pure Ir. The electrochemical experiments were conducted a Biologic VSP-300 potentiostat. A three-electrode cell was used for all experiments. Platinized Pt wire and Reversible Hydrogen Electrode (RHE by Gaskatel) were employed as counter and reference electrodes, respectively. All the reported potentials in the main text and supporting information are referenced to the RHE. The ohmic drop was automatically compensated at 85 % using ZIR method as implemented in EC-lab (Bio-logic, France) interface. The cell resistance was obtained using electrochemical impedance at the high-frequency intercept at 100 kHz (amplitude 10 mV).

IrO_x was investigated as electrodeposited on gold foil. Gold foil was prepared by electrochemical roughening using a method highlighted by Liu et. al.[1] The electrode was cycled from -0.08 to 1.42 V in 0.1 M NaCl. The electrode was held at -0.08 V for 10 s and at 1.42 V for 5s during each cycle. The scan rate was 500 mV/s for 25 cycles. The electrode was then cycled in 0.1 M $HClO_4$ from -0.2 to 2.1 V with scan rate 500 mV/s for 200 cycles. Method highlighted by Mallouk et al was used to prepare the solution for electrodeposition.[2] The solution of IrO_x (10 mM) was prepared by dissolving the precursor (H_2IrCl_6) in 0.5 M NaOH and heating it 90°C for 20 minutes. Finally, a blue colored solution was obtained which was used for depositing IrO_x on Au. For electrodeposition, the potential was held at 1.5 V for 5 min. The electrodeposition process can essentially be described as electrocoagulation (acid condensation) of IrO_x monomers to form polymeric species under acidification near the electrode surface.

For the in situ SERS experiments, the potential was maintained for 30 s at each potential step (0.1 V) and Raman spectra were collected for 10 s. Experiments of IrO_x/Au were conducted in *situ* Raman cell, using a Biologic VSP-300 potentiostat. Raman spectra were collected by Ocean Optics QE65 pro spectrometer using 785 nm Laser source. Laser intensity was maintained at 500 mW (at the source), which was focused on a spot size of 0.1 mm^2. One mm of the electrolyte was always maintained on top of the electrode during all experiments. Sample degradation due to heating from the Laser could be easily ruled in submerged samples. Effect of Au substrate may be non-negligible, but it is a necessary evil as one needs a conducting substrate to electrodeposit the catalyst. Compared to other well-known substrates such as carbon (which corrodes to CO_2 under these potentials), ITO or FTO, Au is relatively inert at potentials of oxygen evolution and allows for consistent interpretation of results. Besides this, a Au substrate allows the possibility of Surface Enhancement for Raman signals

The IrO_x was deposited on a roughened Au foil at 1.5 V for 5 min from 10 mM solution of IrO_x. It was evaluated in NaOH 0.1 M using cyclic voltammetry between 0 - 1.5 V at 100 mV/s. The CV of IrO_x/Au (Figure S1 (a)) is essentially the superposition of CV of pure IrO_x (Figure S1 (c)) and that of bare Au (Figure S1(b)). Peaks (Figure S1 (a)) appearing around 0.65 and 0.9 V correspond to oxidation of Ir.[2] Oxidation peak at around 1.3 V belongs to the oxidation of the Au substrate. The reduction peak at 1.05 V shows the reduction of electrochemically formed AuO_x. The onset of oxygen evolution reaction (OER) can be seen at 1.5 V. CV of the electrochemically grown oxide (on Ir foil) and bare Au foil are shown for comparison. The potential region has been divided from region R1 to R4 for the ease of discussion in the main text. It is well known that the redox behavior of these materials is pH dependent as clearly evident in the CVs shown in Figure S1 (c, d). Since the degree of condensation is affected by pH, these materials are likely to be polymerized to different extents with the alkaline electrolyte showing smaller degrees of polymerization. Figure S2 the currents obtained from in-situ experiments on IrO_x in electrolytes of various pH. Alkaline media shows much higher activty for OER.

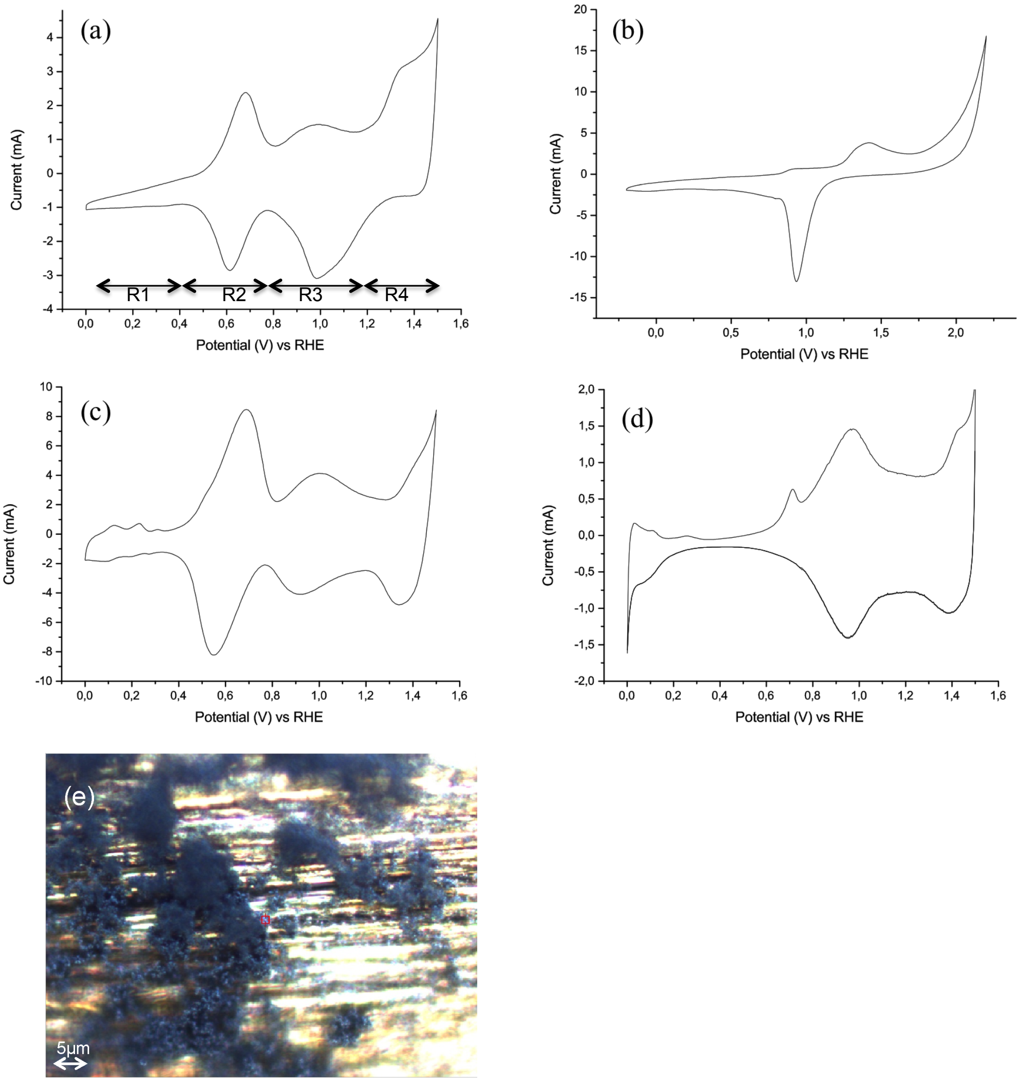

Figure S1: Cyclic voltammograms of (a) IrO_x (on Au foil), (b) bare Au foil and (c) IrO_x (grown on Ir foil) in NaOH 0.5 M at 500 mV/s scan rate; (d) IrO_x (grown on Ir foil) in H_2SO_4 0.5 M at 100 mV/s. (e) Optical microscope image of IrOx/Au deposited at 1.5 V. The laser spot size for Raman spectroscopy is ~0.1 mm^2. This encompasses a large section of the sample that has both pure Au and IrO_x exposed on the sample.

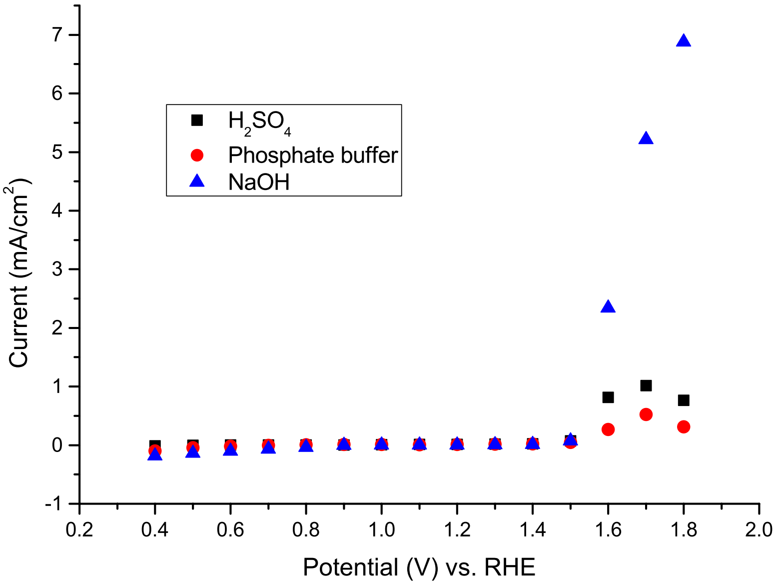

Figure S2: Currents in situ experimental setup of IrO_x*/Au in 0.5 M* H_2SO_4 *(black), 1.0 M phosphate buffer (red) and 0.5 M NaOH (blue) from 0.4–1.8 V. Potential step chronoamperometry was carried out with a step size of 0.1 V for 30 s.*

The *in situ* Raman experiments on IrO_x/Au were also performed in acidic 0.5 M H_2SO_4 media. The potential dependent Raman Spectra are shown in Figure S3. Experiments on Au foil (without IrO_x) are shown in Figure S4. Peaks at 225 cm^{-1} and 316 cm^{-1} originate from the Au surface. Peaks in the range of 445 – 700 cm^{-1} originate from Ir – O stretch vibrations (sometimes coupled to OH bending movements). Although the IrO_x material is present on the Au foil, the over all Raman signal is likely to be a combination of both normal and SERS signals. In our previous publication, using non SERS substrate[3], Ir, the Raman signals at OCP are similar (compared to Figure S3). In the previous publication, we have shown that the chains of edge-sharing octahedral- $[IrO_6]$n provide a good model for describing the anodically formed Ir oxides. These octahedra are linked to each other via μ-oxo type linkages.

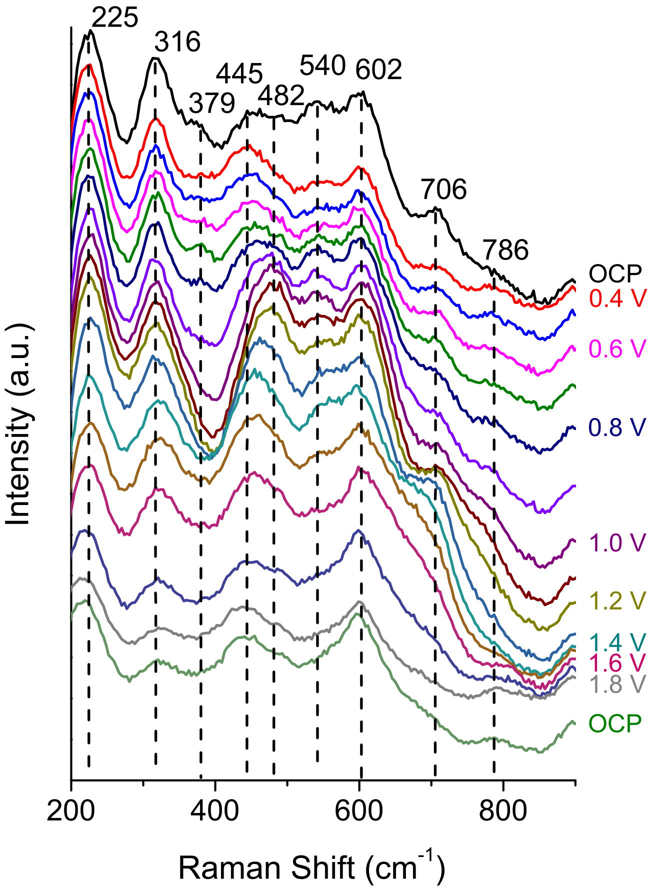

Figure S3: Potential dependent, in situ Raman spectra of IrOx/Au electrode in 0.5 M H_2SO_4.

The overall peak structure of the materials under acidic conditions is not exactly the same, although a three peak pattern between 400 - 700 cm^{-1} can be seen. This happens because the tendency for the IrO_6 octahedra to condense into chains is less in alkaline media. The materials essentially electroprecipitates from the alkaline bath due to local acidity (due to oxidation and creation of protons during OER) at the anode. But once this material is transferred to an acidic electrolyte (e.g. 0.5M H_2SO_4), the material is more robust condensate. The structural behavior is essentially same as that observed in IrOx/Ir-foil. The η peak is visible in acidic medium too but to a much smaller intensity and is very close to 790 cm^{-1} originating from pure Au spectrum (Figure S4(a)). The η peak repoted in Figure 2 have been background corrected. For background correction a linear background connecting anchor points at either side of the peaks was substracted. For representation, the peaks have been normaized to keep the intensity of peak at 316 cm^{-1} same in all spectra. In alkaline media the material has a smaller tendency to condense at high potentials where protons are produced. This allows the material to retain a relatively more open structure in alkaline media and allows for much more active sites resulting in much higher activty (Figure S2). Besides this, the redox peaks of the materials are known to respond to pH which is clearly reflected in the CVs shown in Figure S1.

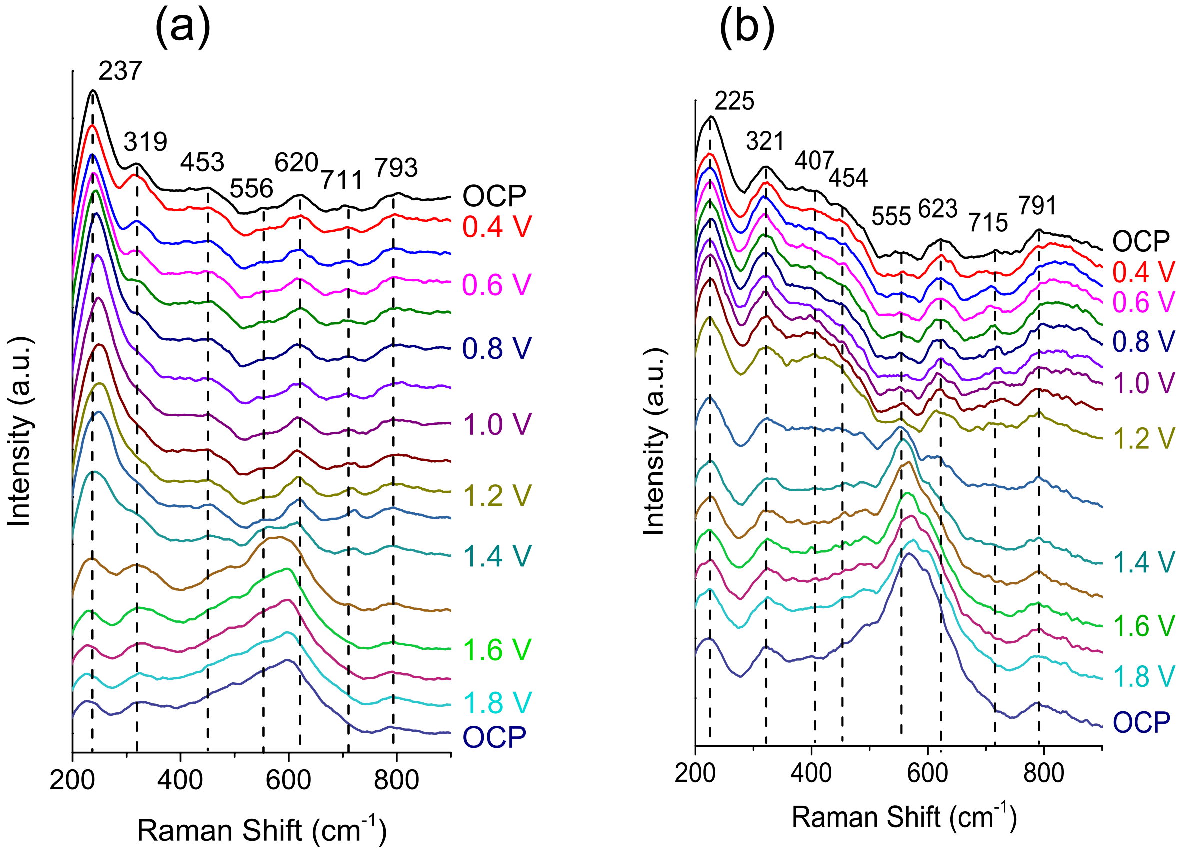

Figure S4: In situ Raman experiments of clean Au foil in 0.5 M H_2SO_4 *(a) and 0.5 M NaOH (b), under the potential regime of 0.4-1.8 V. Potential step of 0.1 V, Raman spectra collection time 10 s.*

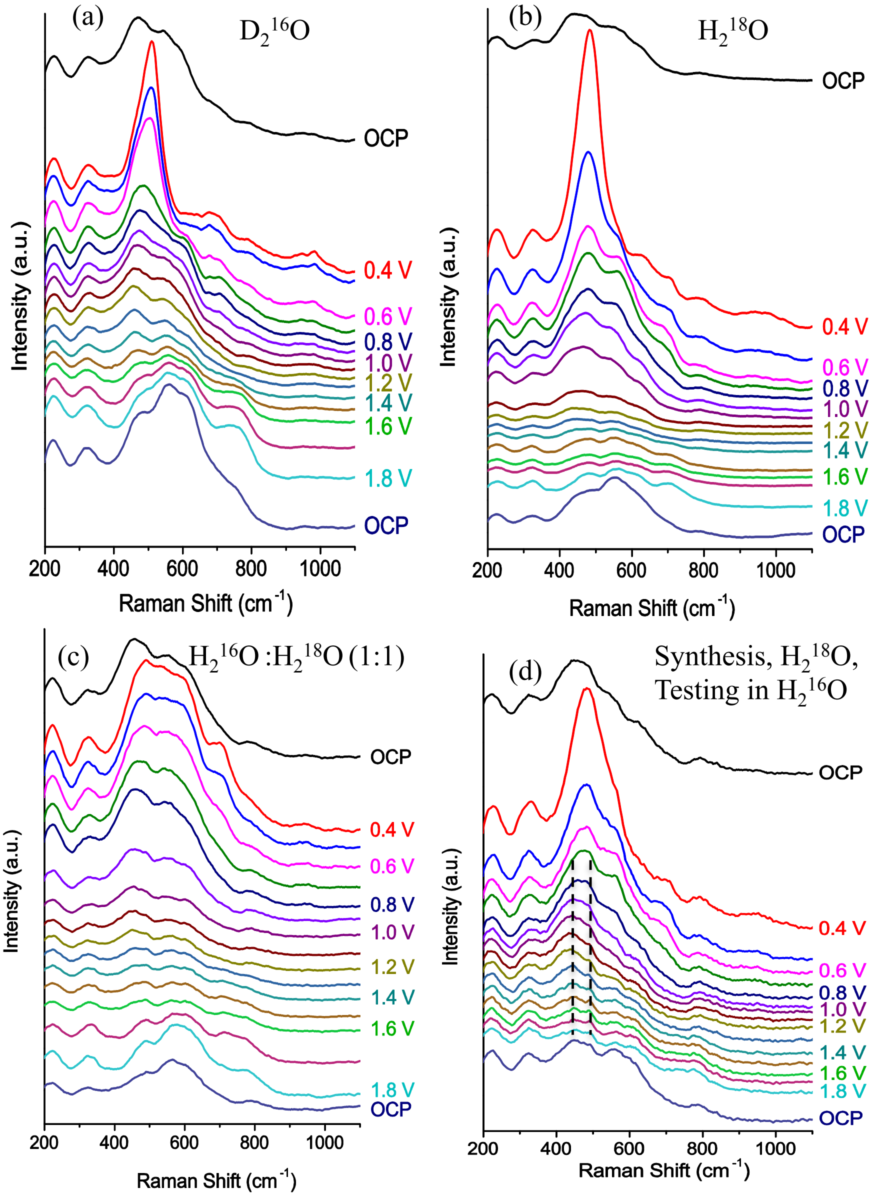

Figure S5: In situ Raman experiments of IrO_x/Au in 0.5 M NaOH, under the potential regime of 0.4-1.8 V, potential step 0.1 V, collection time 10 s. Electrodeposition, as well as testing of IrO_x, are done in the same electrolyte, (a) D_2O^{16}, (b) H_2O^{18}, and (c) H_2O^{16}:H_2O^{18} = 1:1. (d) IrO_x was electrodeposited in H_2O^{18} and tested in H_2O^{16}.

Theoretical Calculations:

All calculations have been performed with the ORCA program package.[4]
Geometry optimizations of trimeric model systems were carried out by using starting structures constructed by hand For this purpose, a bis (μ-O^{2-}) bridged linear chain of three low-spin Ir(IV) atoms was built, which was saturated for each Ir to octahedral geometry by adding water molecules and two hydroxides on each terminal Ir(IV) in order to balance the total charge. The calculations employ the BP86 functional[5] together with the def2-SVP basis set[6-7] and the resolution of identity (RI) approximation. Relativistic corrections were taken into account in zero-th order regular approach.[8-9] Calculations of the Raman spectra have been performed as implemented in ORCA. In order to crudely simulate the effect of surface modification, a water molecule on the middle Ir^{4+} has been replaced by either an oxo or hydroperoxo entity. Optimization of these structures rendered the central Ir^{4+} to be 5-coordinate with an approximate trigonal bi-pyramidal coordination geometry (Figure S6-S8).

$Ir_3O_{14}H_{16}$ (All Ir^{4+} cluster)

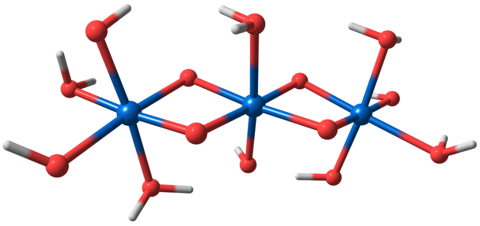

Cartesian Coordinates:

O	-0.567671000	-0.422486000	-1.180306000
O	0.538457000	-0.318831000	1.008905000
O	2.301822000	-1.206230000	-0.696928000
O	-1.908268000	1.076013000	0.912682000
H	-1.528780000	-3.253912000	-0.091911000
H	1.922355000	-1.588620000	0.126463000
H	0.378959000	2.854788000	-0.000065000
O	-0.776524000	-2.895668000	0.412982000
O	-0.101465000	2.182307000	-0.498755000
Ir	1.077533000	0.482260000	-0.706408000
Ir	-1.321736000	-0.837399000	0.599227000
H	2.631622000	1.697606000	-2.216370000
H	1.957740000	0.772238000	-3.297951000
O	1.776935000	1.408778000	-2.596083000
O	-2.050795000	-1.478333000	2.374446000
H	3.104741000	-0.711482000	-0.416077000
H	-1.682442000	1.220542000	1.842678000
O	2.909932000	1.301730000	-0.293384000
H	3.015813000	1.631993000	0.603631000
O	-3.103812000	-1.456414000	0.132489000
Ir	-3.909274000	-1.751252000	1.869354000
O	-5.743219000	-1.935122000	1.185169000
H	-6.235967000	-2.652323000	1.600080000
H	-0.898849000	1.862098000	0.075041000
O	-4.665612000	-2.127383000	3.908206000
H	-4.028700000	-1.747213000	4.528710000
H	-4.411404000	-3.074592000	3.784808000
O	-3.599842000	-3.697539000	2.199305000
H	-2.699257000	-3.751498000	2.548761000
O	-4.402633000	0.339618000	1.628281000
H	-3.640572000	0.747963000	1.145415000
H	-5.158285000	0.269269000	1.023539000
H	-0.957515000	-3.144468000	1.339209000

$Ir_3O_{14}H_{15}$ (OXO) (All Ir^{4+} cluster) Charge= -2, Spin Multiplicity (2S+1)=2

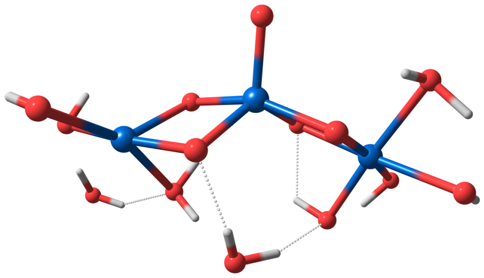

O	-1.340503000	0.394446000	-0.893689000
O	0.149248000	0.821433000	1.017758000
O	0.975354000	-1.176260000	-0.076400000
O	-2.377000000	2.236265000	1.410330000
H	-1.540102000	-1.401215000	-1.220835000
H	0.197309000	-1.718210000	-0.444528000
H	1.507839000	2.548732000	-2.137816000
O	-1.234936000	-2.343164000	-1.120484000
O	0.585043000	2.200393000	-2.225783000
Ir	0.639405000	0.835001000	-0.901765000
Ir	-1.845229000	0.624841000	0.907393000
H	3.577195000	-0.045732000	-0.707079000
H	3.097439000	-1.430684000	-0.377710000
O	3.941514000	-0.968679000	-0.546616000
O	-1.868380000	-0.700089000	2.259204000
H	0.658192000	-0.791358000	0.806455000
O	2.631734000	1.407830000	-0.833544000
H	2.700491000	1.814348000	0.048940000
O	-3.630241000	-0.235305000	0.578866000
Ir	-3.641713000	-1.627001000	1.984842000
O	-5.540726000	-2.423657000	1.614208000
H	-5.643055000	-3.106448000	2.302143000
O	-3.469561000	-3.344103000	3.527277000
H	-2.917698000	-2.807682000	4.125853000
H	-2.834034000	-3.592818000	2.736628000
O	-2.339205000	-3.090773000	1.344647000
H	-1.494378000	-2.634041000	1.562277000
O	-5.109821000	-0.178972000	2.589432000
H	-4.843032000	0.328570000	1.754859000
H	-5.747061000	-0.912806000	2.247613000
H	-1.803475000	-2.692358000	-0.384451000

$Ir_3O_{15}H_{15}$ (OXO) (All Ir^{4+} cluster) Charge= -1, Spin Multiplicity (2S+1)=2

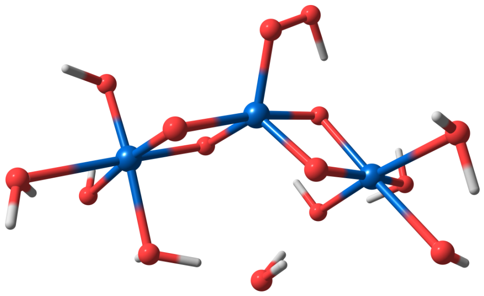

O	-0.793295000	0.983098000	-0.872834000
O	0.067357000	0.163684000	1.252367000
O	0.859852000	-1.481605000	-1.037988000
O	-2.440304000	2.288923000	1.326612000
H	-1.857025000	-2.310106000	-0.421620000
H	0.061328000	-2.015815000	-0.596128000
H	1.724859000	2.879890000	-0.527755000
O	-1.081008000	-2.831620000	-0.118644000
O	1.506193000	2.345726000	0.259635000
Ir	1.030333000	0.573342000	-0.421677000
Ir	-1.702368000	0.631896000	0.902827000
H	2.957145000	0.526294000	-1.575355000
H	1.968187000	0.288967000	-2.844670000
O	2.246812000	0.974349000	-2.209726000
O	-2.550973000	-0.008246000	2.673706000
H	1.681697000	-1.787977000	-0.599943000
O	2.999649000	-0.138683000	-0.189394000
H	3.400940000	0.339301000	0.555945000
O	-2.900047000	-0.647850000	0.223292000
Ir	-3.585109000	-1.535916000	1.830205000
O	-4.735513000	-2.968579000	0.782685000
H	-5.051505000	-3.621790000	1.431095000
O	-3.998943000	-2.562144000	3.726979000
H	-3.979758000	-1.806344000	4.345363000
H	-3.012398000	-2.817025000	3.595296000
O	-1.873091000	-2.488114000	2.414023000
H	-1.386757000	-1.700044000	2.764747000
O	-5.464051000	-0.728679000	1.203476000
H	-5.205566000	-0.161468000	0.448117000
H	-5.519960000	-1.747168000	0.825674000
H	-1.236271000	-2.804759000	0.883329000
O	-3.029879000	2.406234000	2.671349000
H	-3.015022000	1.364072000	2.897887000

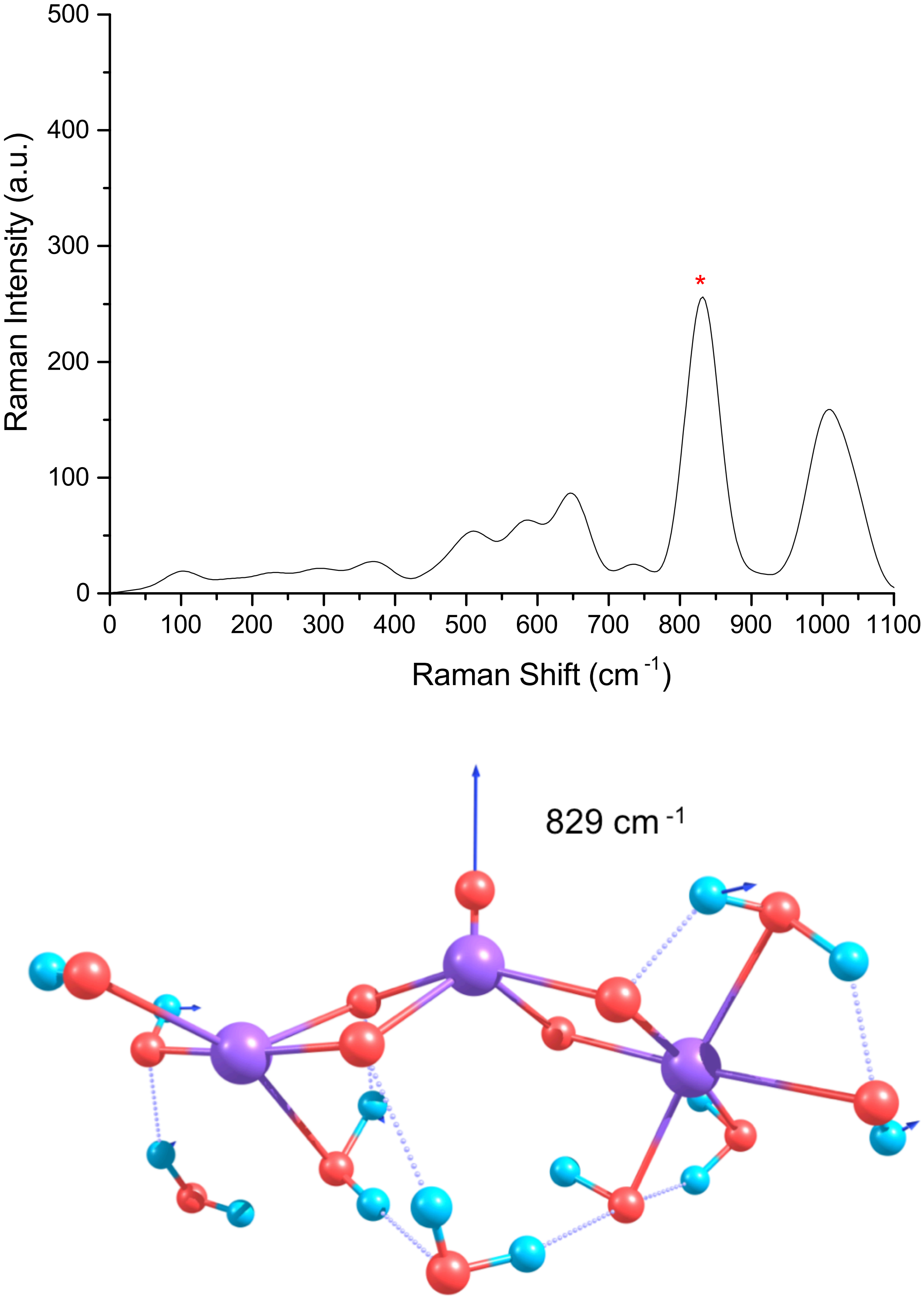

Figure S6: Computed Raman spectrum for the IrOx-oxo species. The Ir-O stretch vibration for the oxo species is very strong and located at 829 cm^{-1}. The vibration is shown with arrows. The size of the arrows shows the relative contribution of various movements to the overall mode.

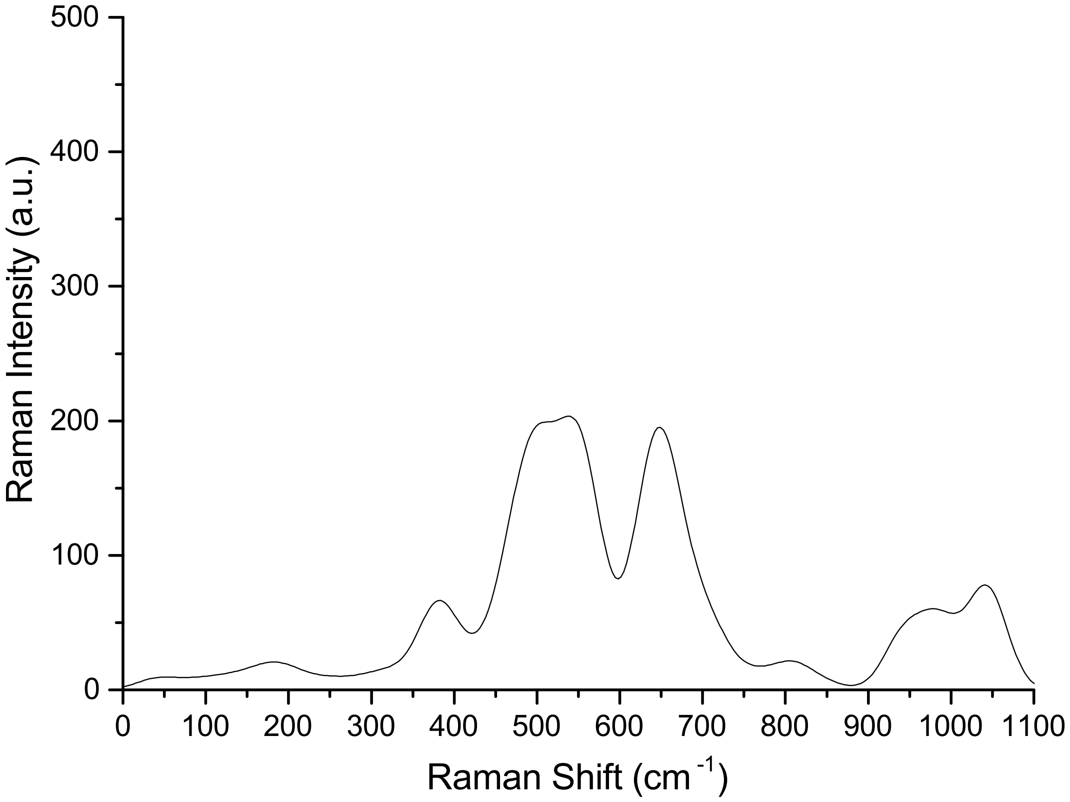

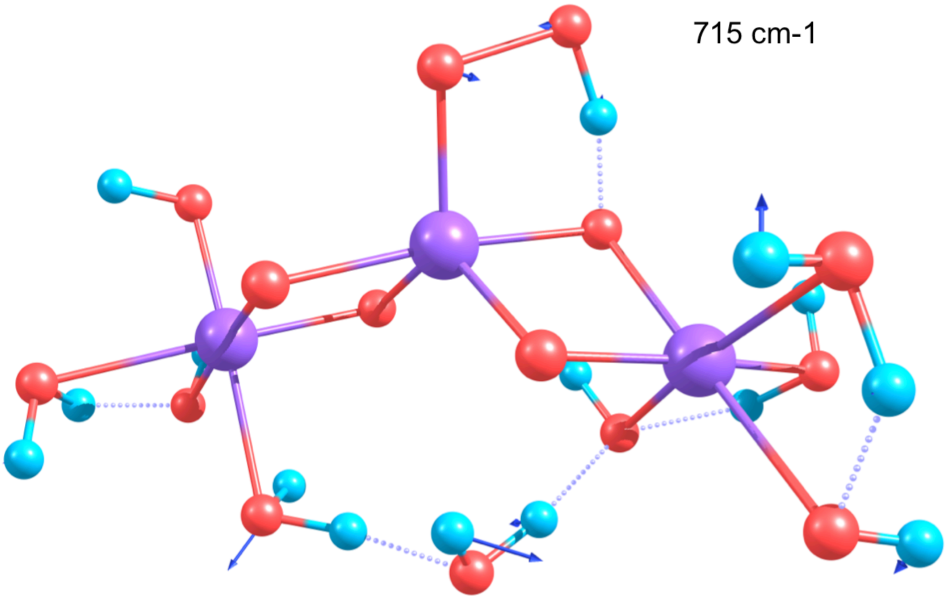

Figure S7: Computed Raman spectrum for the IrOx-peroxo species. The O-O stretch vibration for the peroxo species is located at 715 cm^{-1}. The intensity of this mode is minor compared other Raman active modes.

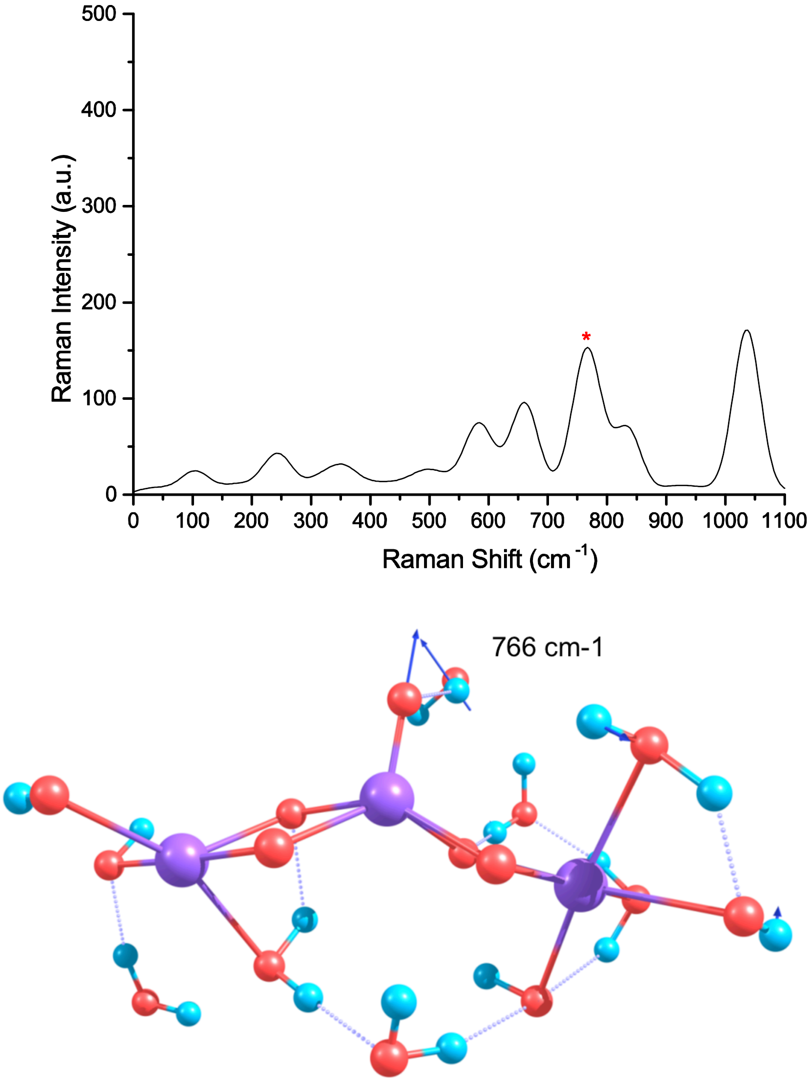

Figure S8: Computed Raman spectrum for the IrOx-oxo with a water molecule near the Ir-O species. The Ir-O stretch vibration tends to couple with the OH bend of the water molecule which can drag it down to 766 cm^{-1}*. The vibration is shown with arrows. The size of the arrows shows the relative contribution of various movements to the overall mode.*

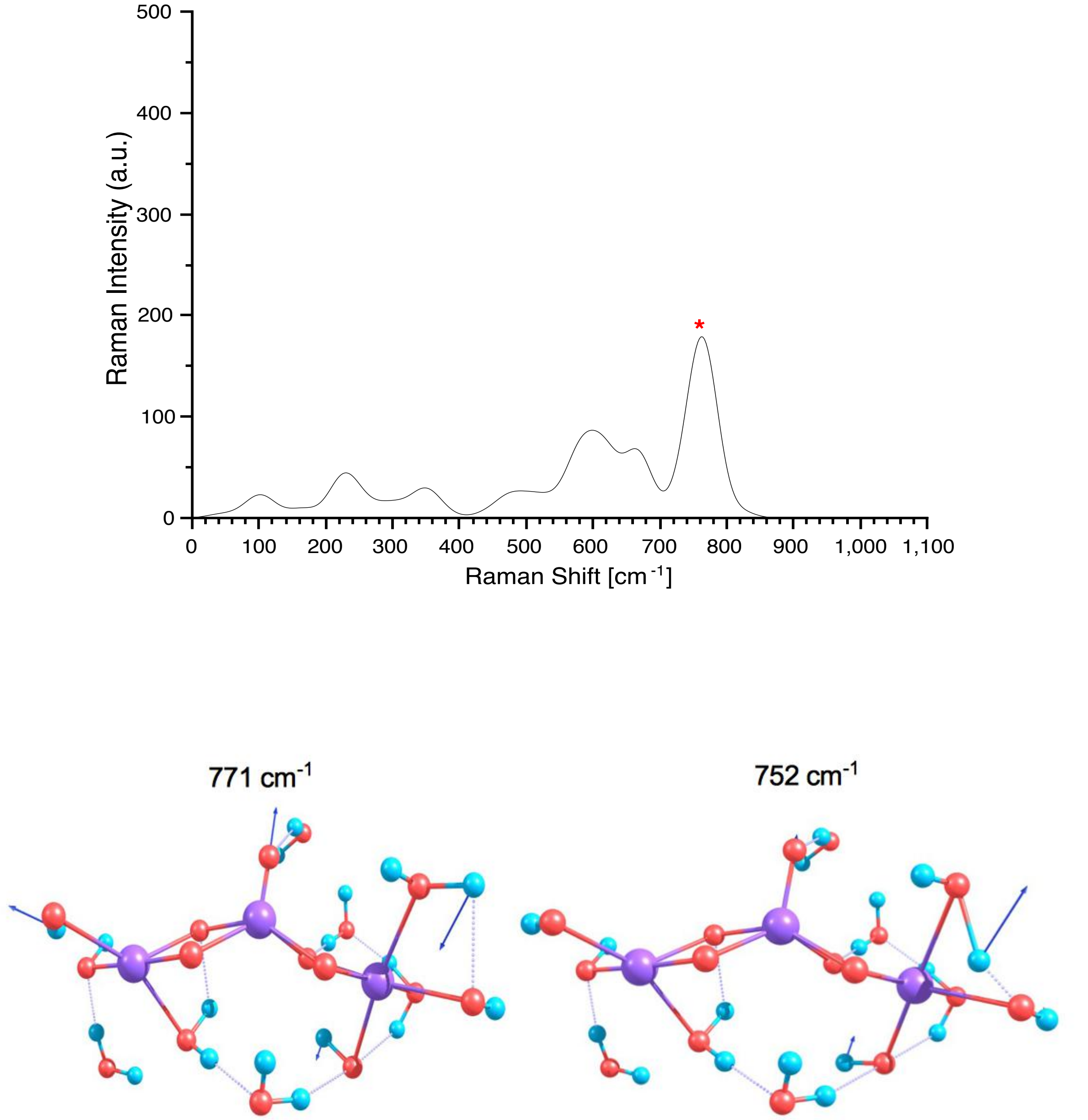

Figure S9: Computed Raman spectrum for the IrO$_x$-oxo with a D$_2$O molecule near the Ir-O species. Unlike Figure S8, The Ir-O stretch vibration is not coupled to OD bend but the strong signal is split into 771 and 752 cm^{-1} with the former having most of the Ir-O stretch character. The vibration is shown with arrows. The size of the arrows shows the relative contribution of various movements to the overall mode. Thus, inspite of D$_2$O substitution, the overall IrO$_x$-oxo vibration remains around 771 cm^{-1}.

References:

---

1. Liu, Y. C.; Wang, C. C.; Tsai, C. E., Effects of electrolytes used in roughening gold substrates by oxidation-reduction cycles on surface-enhanced Raman scattering. *Electrochem Commun* **2005,** *7* (12), 1345-1350.
2. Zhao, Y. X.; Vargas-Barbosa, N. M.; Hernandez-Pagan, E. A.; Mallouk, T. E., Anodic Deposition of Colloidal Iridium Oxide Thin Films from Hexahydroxyiridate(IV) Solutions. *Small* **2011,** *7* (14), 2087-2093.

3. Zoran Pavlovic, Chinmoy Ranjan, Qiang Gao, Maurice van Gastel, and Robert Schlögl, *ACS Catal.*, 2016, 6 (12), 8098–8105.

4. Neese, F. The ORCA Program System. *Wiley Interdiscip. Rev. Comput. Mol. Sci.* **2012**, *2*, 73–78.

5. Becke, A. D. Density-Functional Exchange-Energy Approximation with Correct Asymptotic Behavior. *Phys. Rev. A* **1988**, *38*, 3098–3100.

6. Eichkorn, K.; Weigend, F.; Treutler, O.; Ahlrichs, R. Auxiliary Basis Sets for Main Row Atoms and Transition Metals and their Use to Approximate Coulomb Potentials. *Theor. Chem. Acc.* **1997**, *97*, 119–124.

7. Eichkorn, K.; Treutler, O.; Öhm, H.; Häser, M.; Ahlrichs, R. Auxiliary Basis Sets to Approximate Coulomb Potentials. *Chem. Phys. Lett.* **1995**, *240*, 283–290.

8. E. van Lenthe, J. G. Snijders, E. J. Baerends, *J. Chem. Phys.* **1996**, *105*, 6505-6516.

9. E. van Lenthe, A. van der Avoird, P. E. S. Wormer, *J. Chem. Phys.* **1998**, *108*, 4783-4796.